ORIGINAL RESEARCH ARTICLE

WILEY *Journal of Cellular Physiology*

hiPSC-derived hepatocytes closely mimic the lipid profile of primary hepatocytes: A future personalised cell model for studying the lipid metabolism of the liver

Mostafa Kiamehr[1] | Anna Alexanova[1] | Leena E. Viiri[1] | Laura Heiskanen[2] | Terhi Vihervaara[2] | Dimple Kauhanen[2] | Kim Ekroos[5] | Reijo Laaksonen[1,2] | Reijo Käkelä[3] | Katriina Aalto-Setälä[1,4]

[1]Faculty of Medicine and Life Sciences, University of Tampere, Tampere, Finland

[2]Zora Biosciences, Espoo, Finland

[3]Faculty of Biology and Environmental Sciences, University of Helsinki, Helsinki, Finland

[4]Heart Hospital, Tampere University Hospital, Tampere, Finland

[5]Lipidomics Consulting Ltd, Espoo, Finland

Correspondence
Mostafa Kiamehr, Faculty of Medicine and Life Sciences, University of Tampere, Tampere, Finland.
Email: mostafa.kiamehr@uta.fi

Abstract

Hepatocyte-like cells (HLCs) differentiated from human-induced pluripotent stem cells offer an alternative platform to primary human hepatocytes (PHHs) for studying the lipid metabolism of the liver. However, despite their great potential, the lipid profile of HLCs has not yet been characterized. Here, we comprehensively studied the lipid profile and fatty acid (FA) metabolism of HLCs and compared them with the current standard hepatocyte models: HepG2 cells and PHHs. We differentiated HLCs by five commonly used methods from three cell lines and thoroughly characterized them by gene and protein expression. HLCs generated by each method were assessed for their functionality and the ability to synthesize, elongate, and desaturate FAs. In addition, lipid and FA profiles of HLCs were investigated by both mass spectrometry and gas chromatography and then compared with the profiles of PHHs and HepG2 cells. HLCs resembled PHHs by expressing hepatic markers: secreting albumin, lipoprotein particles, and urea, and demonstrating similarities in their lipid and FA profile. Unlike HepG2 cells, HLCs contained low levels of lysophospholipids similar to the content of PHHs. Furthermore, HLCs were able to efficiently use the exogenous FAs available in their medium and simultaneously modify simple lipids into more complex ones to fulfill their needs. In addition, we propose that increasing the polyunsaturated FA supply of the culture medium may positively affect the lipid profile and functionality of HLCs. In conclusion, our data showed that HLCs provide a functional and relevant model to investigate human lipid homeostasis at both molecular and cellular levels.

- -

1 | INTRODUCTION

The liver plays an important role in the regulation of many physiological functions of the body, including lipid and carbohydrate metabolism, glycolytic/urea metabolism, plasma protein synthesis, and the detoxification of a wide variety of molecules (Si-Tayeb et al., 2010). Hepatocytes, which comprise about 70% of the liver's mass, originate from the anterior portion of the definitive endoderm (DE), one of the three embryonic layers (Blouin, Bolender, & Weibel, 1977). Hepatocytes handle many crucial metabolic functions of the liver, including the synthesis of lipoproteins, triacylglycerols (TAGs), cholesterol, and phospholipids (PLs; Gordillo, Evans, & Gouon-Evans, 2015).

Primary human hepatocytes (PHHs) are currently considered the "gold standard" in cell modeling for studying, for example, liver physiology, toxicity, and lipid homeostasis. Typically, PHHs are obtained from cadaveric donors, but they are scarce and functionally heterogeneous, and it is hard to maintain them in a culture. When cultured, PHHs loose functionality relatively fast, and their liver-specific features progressively deteriorate, which particularly hampers long-term studies (Elaut et al., 2006; Godoy et al., 2013). To address these limitations, various human hepatoma cell lines, including HepG2 and Huh7, have been used due to their ease of handling, unlimited life span, and stable phenotype. Nevertheless, they do not faithfully mirror the metabolic activities of healthy liver cells. In fact, the expression levels and profiles of genes involved in liver-specific functions are poorly presented in these systems (Olsavsky et al., 2007). As a result, hepatoma cell lines have failed to predict the numerous adverse hepatotoxic side effects of new drugs (Castell, Jover, Martínez-Jiménez, & Gómez-Lechón, 2006). Alternatively, animal models, such as rats and mice, or animal primary hepatocytes have been widely used to study lipid metabolism and lipoprotein production in the liver (Kvilekval, Lin, Cheng, & Abumrad, 1994). However, the information gained from murine cells is not fully translatable to humans, and there are significant differences in lipid metabolism between the species. Animal models are also expensive and unsuitable for large-scale screening. Furthermore, due to growing ethical concerns, there is an urgent need to reduce the use of rodents and other animal models in research.

Human-induced pluripotent stem cells (hiPSCs) provide an unlimited supply of tissue-specific differentiated cell types for disease modeling and cell therapy. Hepatocytes differentiated from pluripotent stem cells circumvent the problem of the limited availability of cells faced when working with PHHs. They show very similar characteristics to PHHs; for instance, they secrete albumin as well as urea, and to some extent express drug transporters and cytochrome P450 enzymes (Kia et al., 2012). Unlike rodent hepatocytes and some human hepatoma cells, these hepatocyte-like cells (HLCs) are sensitive to hepatitis C virus infection and support viral replication similar to PHHs (Schwartz et al., 2012). Patient-specific iPSC lines provide us with an advantageous system of HLCs from patients of different genetic backgrounds, a prerequisite for the development of personalised medicine. The generation of hiPSC-derived HLCs (hiPSC-HLCs) in large quantities enables their use in modeling inborn errors of hepatic metabolism, understanding the molecular basis of liver cell differentiation, studying disease mechanisms, and facilitating drug discovery and safety. HLCs have already proven to be of great value in developing novel therapeutics (Medine et al., 2013; Szkolnicka et al., 2014) and identifying the noncoding micro-RNAs regulating human liver damage (Szkolnicka et al., 2016; Yang et al., 2016). HLCs have also been successfully used as in vitro cell culture systems, for example, to recapitulate the pathophysiology of familial hypercholesterolemia (Cayo et al., 2012) and human cholesterol homeostasis (Krueger et al., 2013). Lipid defects are central to the pathogenesis of many common diseases, such as atherosclerosis (Meikle et al., 2011; Stübiger et al., 2012) and nonalcoholic fatty liver disease (Ruhanen et al., 2017; Younossi et al., 2016). Therefore, hiPSC-HLCs offer a great platform for investigating the basic mechanisms of lipid metabolism and its dysregulation in a patient-specific manner. However, to date, no detailed studies have yet been performed on the lipid profile and fatty acid (FA) metabolism of HLCs. To better use HLCs as a cell model to study the role of molecular lipids in liver diseases, it is essential to know their lipid profile in relation to actual human adult liver tissue and to the currently used cell models, namely PHHs and hepatoma cell lines.

Hepatic differentiation methods have greatly improved over the last decade, enabling the efficient generation of high quality HLCs from pluripotent stem cells (Cameron et al., 2015; Hannan, Segeritz, Touboul, & Vallier, 2013; Hay et al., 2008; Kajiwara et al., 2012; Si-Tayeb et al., 2010). Nevertheless, the experimental details and some differentiation factors differ between the current protocols, which might affect the phenotype of the HLCs. To reproduce the physiological conditions of the human liver, it is crucial to generate functional HLCs that are as similar as possible to PHHs. In this study, we describe five protocols for generating HLCs from hiPSCs and comprehensively compare the morphology, genetics, biochemistry, and functional traits of the HLCs produced. In addition, we compare the HLCs with the two most common cell models currently used—PHHs and HepG2 cells—as well as human liver tissue. Most importantly, the lipid profiles of HLCs, PHHs, and HepG2 cells are analyzed by both mass spectrometry (MS) and gas chromatography, and the similarities and main differences between the cell types are discussed in light of selected key genes involved in FA metabolism. Finally, the lipid profile of HLCs is fully characterized, and the potential and

limitations of HLCs as a model for studying lipid metabolism are evaluated.

2 | MATERIAL AND METHODS

2.1 | Ethical issues

The study and patient recruitment have been approved by the Ethics Committee of Tampere University Hospital (approval number: R12123). All participants providing skin biopsies were adults more than 18 years old who had signed an informed consent form after receiving both oral and written descriptions of the study.
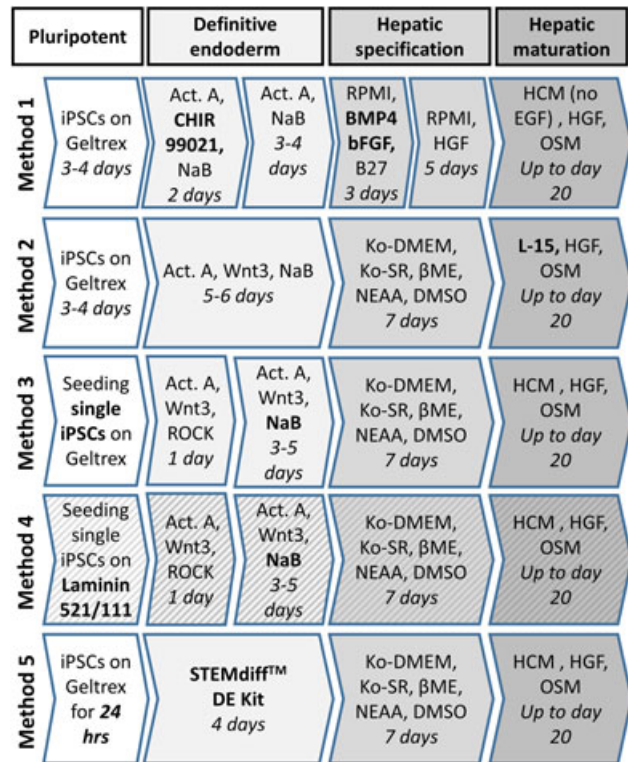
2.2 | hiPSC reprogramming and cell culture

Three hiPSC lines (UTA.10100.EURCAs, UTA.11104.EURCAs, and UTA.11304.EURCCs) were generated directly from the fibroblasts of three individuals. Pluripotency was induced with the Sendai reprogramming kit (OCT4, SOX2, KLF4, C-MYC; CytoTune; Life Technologies, USA) based on the protocol described by Ohnuki, Takahashi, Yamanaka, (2009) and Takahashi & Yamanaka, (2006). hiPSCs were then maintained as described before (Kiamehr et al., 2017). Details of the hiPSC cell culture are also described in the Supporting Information.

2.3 | Hepatic differentiation

In all methods except Method 4 (M4), hiPSCs were transferred from mouse embryonic fibroblasts to Geltrex™ (USA; Cat: A14133-01, 1:50 dilution), kept in mTeSR1™ medium, and adapted to the changed culture conditions for a few passages before commencing the differentiation. In M4, hiPSCs were adapted on Laminin 521 (BioLamina, Lot: 80104) first, and the differentiation was completed on Laminin mix 111/521-coated plates (3:1 ratio, 10 μg/ml). The hiPSCs used in all methods were at passage 20 or higher before commencing the differentiation. Three lines were differentiated using each method, except Method 5 (M5), which was applied to two cell lines. Figure 1 shows a schematic view of all five methods used in the study. Details of the five differentiation methods are described in detail in the Supporting Information.

2.4 | PHHs and HepG2 cells

Cryopreserved PHHs (Cat. No. HMCPIS, Lot. HU8210, USA) were purchased from Gibco®, and hepatocellular carcinoma cells (HepG2, ATCC-HB-8065, Lot. No. 59947519) were purchased from ATCC™. Both cells were plated according to the manufacturer's instructions. PHHs were cultured in William's E medium (A1217601, Gibco, USA) supplemented with cocktail B (Gibco, CM 4000) and dexamethasone, whereas the HepG2 cells were cultured in Dulbecco's modified Eagle medium supplemented with 10% FBS.

	Pluripotent	Definitive endoderm		Hepatic specification		Hepatic maturation
Method 1	iPSCs on Geltrex 3-4 days	Act. A, **CHIR 99021**, NaB 2 days	Act. A, NaB 3-4 days	RPMI, **BMP4 bFGF**, B27 3 days	RPMI, HGF 5 days	HCM (no EGF), HGF, OSM *Up to day 20*
Method 2	iPSCs on Geltrex 3-4 days	Act. A, Wnt3, NaB 5-6 days		Ko-DMEM, Ko-SR, βME, NEAA, DMSO 7 days		**L-15**, HGF, OSM *Up to day 20*
Method 3	Seeding **single iPSCs** on Geltrex	Act. A, Wnt3, ROCK 1 day	Act. A, Wnt3, **NaB** 3-5 days	Ko-DMEM, Ko-SR, βME, NEAA, DMSO 7 days		HCM, HGF, OSM *Up to day 20*
Method 4	Seeding single iPSCs on **Laminin 521/111**	Act. A, Wnt3, ROCK 1 day	Act. A, Wnt3, **NaB** 3-5 days	Ko-DMEM, Ko-SR, βME, NEAA, DMSO 7 days		HCM, HGF, OSM *Up to day 20*
Method 5	iPSCs on Geltrex for **24 hrs**	STEMdiff™ DE Kit 4 days		Ko-DMEM, Ko-SR, βME, NEAA, DMSO 7 days		HCM, HGF, OSM *Up to day 20*

FIGURE 1 A schematic representation of the five hepatic differentiation protocols used for generating hepatocyte-like cells (HLCs). Differentiation in Method 1 and Method 2 (M1 and M2) were started with hiPSC colonies, in Method 3 and Method 4 (M3 and M4) with dissociated iPSC single cells, and in Method 5 (M5) with 24 hrs post-cultured hiPSCs. Plates in Method 4 (M4) were coated with a mix of Laminin 111/521 (3:1 ratio) instead of the Geltrex™ used in the remainder of the methods. hiPSC: human-induced pluripotent stem cell [Color figure can be viewed at wileyonlinelibrary.com]

2.5 | RT-polymerase chain reaction

RNA extraction and polymerase chain reaction (PCR) for pluripotency markers (*OCT4*, *NANOG*, *SOX2*, and *SSEA4*) were performed as published before (Manzini, Viiri, Marttila, & Aalto-Setälä, 2015).

2.6 | Quantitative PCR (qPCR) analysis

RNA samples were collected at the hiPSC, DE, and HLC stages, and RNA was extracted using an RNeasy kit (Qiagen, Germany, Cat. No. 74106). Complementary DNA (cDNA) was generated using a high capacity cDNA Reverse Transcription kit (Applied Biosystems) according to the manufacturer's instructions in the presence of an RNase inhibitor. cDNA was multiplied either by the Power SYBR Green PCR Master Mix (Life Technology, Cat. No. 1408470, Austin, TX) and gene-specific primers (*OCT4*, *SOX17*, *FOXA2*, *AFP*, *ALB*) or by the TaqMan Universal Master Mix (Applied Biosystems, 4304437, Austin, TX) and gene-specific TaqMan probes (*APOA1*, *APOB*, *FADS1*, *FADS2*, *ELOVL2*, *ELOVL5*, *FASN*) using the BioRad CFX384 Real-Time PCR Detection System. Values were normalized to *GAPDH*, which was used as an endogenous control, and relative quantification was

calculated by the ΔΔCT method (Livak & Schmittgen, 2001). PHH was used as the reference sample.

First Choice® Human Liver Total RNA (hLTR, Cat. No. AM7960), purchased from Ambion®, was used as an extra control. The results from qPCR were compared for the HLCs and the three reference samples (PHHs, hLTR, and HepG2 cells).

2.7 | Immunostaining

Cells were fixed, stained, and visualized as described before (Kiamehr et al., 2017). Details are also provided in the Supporting Information. The percentage of ALB-positive cells and binuclear HLCs were calculated manually by counting HLCs in 3–5 stained areas and calculating the average.

2.8 | low-density lipoprotein uptake

The ability of the cells to uptake low-density lipoprotein (LDL) was evaluated by incubating the HLCs with labeled LDL (Cell-based assay kit, Cayman, USA, Cat. No. 10011125) for 4 hr, after which the cells were imaged by fluorescent microscopy.

2.9 | FACS analysis

To analyze the number of CXCR4-positive cells, endodermal cells were detached with Versene (Gibco®, UK), suspended in 3%–5% bovine serum albumin buffer, stained with a PE-conjugated CXCR4 antibody (R&D Systems FAB173P, Minneapolis, 10 μl for 10^6 cells) for 15 min at RT, washed three times, and analyzed using the Accuri™ C6 device (BD Biosciences).

2.10 | Albumin, urea, and TAG secretion

At the late stage of hepatic differentiation, HLCs were evaluated for their functionality. The albumin, urea, and TAG content of the conditioned medium were determined, respectively, with the Human Albumin ELISA Quantitation kit (Bethyl Laboratory), the Quanti-Chrom™ Urea Assay Kit (BioAssay Systems, USA), and the Triglyceride Quantification Kit (BioVision Inc., Cat. No. K622-100, USA) according to the manufacturers' instructions. The values were normalized to cell numbers. The results were then compared with the data from the PHHs and HepG2 cells, which were cultured in parallel with the HLCs.

2.11 | Lipid mass spectrometry

2.11.1 | Lipid sample preparation and extraction

Lipids (sphingolipids [SL], cholesterol, glycerolipids, and glycerophospholipids) were extracted from the HLCs by Hamilton Robotics AB and studied by shotgun lipidomics. The detailed procedure is described by Kiamehr et al., (2017).

2.11.2 | Mass spectrometric analyses and data processing

In the shotgun lipidomics (cholesteryl ester [CE], diacylglycerol [DAG], sphingomyelin [SM], lysophosphatidylcholine [LPC], lysophosphatidylethanolamine [LPE], lysophosphatidylserine, lysophosphatidylglycerol, and lysophosphatidylinositol [LPI]), lipid extracts were analyzed on a hybrid triple quadrupole/linear ion trap mass spectrometer (QTRAP 5500) equipped with a robotic nanoflow ion source (NanoMate, Advion Biosciences Inc., Ithaca, NJ) as described by Heiskanen, Suoniemi, Ta, Tarasov, & Ekroos, (2013). Molecular lipids were analyzed in positive ion mode using lipid class-specific precursor ion or neutral loss scans (Ekroos, Chernushevich, Simons, & Shevchenko, 2002; Ekroos et al., 2003).

Sphingolipids (ceramide [Cer], glucosyl/galactosylceramide [Glc/GalCer], lactosylceramide [LacCer], and globotriaosylceramide [Gb3]) and molecular PLs (phosphatidylcholines [PC], phosphatidylethanolamines [PE], and phosphatidylinositols [PI]) were analyzed with a targeted approach using ultra-high-pressure liquid chromatography-mass spectrometry (UHPLC-MS; Merrill, Sullards, Allegood, Kelly, & Wang, 2005). An analytical Acquity BEH C18, 2.1×50 mm column with a particle size of 1.7 μm (Waters, Milford, MA) heated to 60°C was used. Mobile phases consisted of 10 mM ammonium acetate in water with 0.1% formic acid (solvent A) and 10 mM ammonium acetate in acetonitrile:isopropanol (4:3, v/v) containing 0.1% formic acid (solvent B). The flow rate was set to 500 μl/min. Sphingolipids were separated with a 15 min linear gradient from 75% B to 100% B, while molecular PLs were analyzed using a 10 min gradient from 75% B to 80% B. Both sphingolipids and PLs were analyzed on a hybrid triple quadrupole/linear ion trap mass spectrometer (5500 QTRAP) equipped with an UHPLC system (CTC HTC PAL autosampler and Rheos Allegro pump or Shimadzu Nexera X2) using a multiple reaction monitoring based method in positive ion mode for sphingolipids and negative ion mode for molecular PLs. Curtain gas was set at 25; the ion spray voltage was set at 5000 V in positive ion mode and −4500 V in negative ion mode, and the ion source was heated to 400°C in positive mode and to 300°C in negative ion mode. The collision energy was optimized for each lipid class. Identified lipids were quantified by normalizing against their respective internal standard (Ejsing et al., 2006) and total protein concentrations in the cell sample. Total protein concentrations were determined using the Micro BCA™ Protein Assay Kit (Thermo Scientific Pierce Protein Research Products) according to the manufacturer's instructions. Data processing was performed by MultiQuant, LipidView (AB Sciex) software and SAS.

2.12 | FA gas chromatography

To confirm our observations from the MS analysis of molecular lipids and to investigate the effect of the medium on the FA profile of the cells, the FA composition of HLCs, PHHs, and HepG2 cells and their media was analyzed by gas chromatography as described in detail by Kiamehr et al., (2017). Briefly, the acyl chains in the cell pellet

lipids or the lipid residues of the nitrogen-dried media were converted to FA methyl esters (FAMEs) in a transesterification reaction with 1% methanolic H_2SO_4. The quantitative analysis of the FAMEs, which were extracted into hexane, was performed using a Shimadzu GC-2010 Plus gas chromatograph with a flame-ionization detector, and the FAME structures were identified by Shimadzu GCMSQP2010 Ultra with a mass selective detector. In both systems, the components of the FAME mixtures were separated in ZB-wax capillary columns (30 m, 0.25 mm ID, 0.25 μm film; Phenomenex). The calculations of the FA compositions and concentrations followed standard procedures (Kiamehr et al., 2017), and the FAs were marked by using the abbreviations: [carbon number]:[number of double bonds] n-[position of the first double bond calculated from the methyl end] (e.g., 22:6n-3).

2.13 | Statistical analysis

GraphPad Prism version 5.02 software was used for the data analysis. Data are presented as means ± standard deviation with n representing the number of independent experiments. The results were compared using one-way analysis of variance, followed by Bonferroni's multiple-comparison test. A p value < 0.05 was considered statistically significant.

3 | RESULTS

3.1 | Cell morphology during hepatic differentiation

In all methods, dramatic morphological changes were observed, particularly during the first few days of DE differentiation. In all methods except M5, migrating DE cells possessed a spiky morphology, whereas in M5, migrating cells were instead more round or square-shaped (Supporting Information Figure S1a). In addition, the amount of cell death in M5 was considerably lower than in the other methods. No morphological differences were observed between the DE cells treated with CHIR 99021 (Method 1, M1) or Wnt3 (Methods 2–4, M2–4). Initiating differentiation with single cells in M3 and M4 did not yield a higher efficiency of DE formation compared with M1 and M2, which were started with colonies (Supporting Information Figures S1a and S3). However, we did observe cells with a DE morphology appearing one or even two days earlier in methods initiated with single cells compared with methods initiated with colonies (Supporting Information Figure S1a). At the hepatic specification stage, cells treated with basic fibroblast growth factor, bone morphogenic protein 4 (BMP4), and hepatocyte growth factor (HGF; M1) clearly had a different morphology compared with the cells treated with DMSO (M2–5; Supporting Information Figure S1b), which might imply different pathways toward hepatoblasts in those protocols.

Binucleation is a feature of adult hepatocytes and generally considered a sign of terminal differentiation (Miyaoka & Miyajima, 2013). We found 29% of the PHHs and on average 10% of the HLCs

to be binuclear (Figures 1b and 2a). The HLCs differentiated by M4 showed the closest binuclearity (16%) to the PHHs. No individual cell line was shown to be more potent in generating binuclear cells.

3.2 | Characterization of DE and HLCs at the protein level

hiPSCs expressed OCT4 protein, which was lost during the DE stage, while the expression of DE markers SOX17 and FOXA2 was upregulated (Supporting Information Figure S2a). The efficiency of the DE differentiation, estimated by measuring the CXCR4 expression by flow cytometry, did not differ across M1, M2, and M3 (Supporting Information Figure S2b). In M4 and M5, the amount of CXCR4-positive cells was lower than in the other methods.

The immature hepatic marker AFP was expressed in hepatic progenitor cells and remained expressed until the later stages in all five methods (Figure 2a). In addition, ALB, LDL receptor (LDL-R), and asialoglycoprotein receptor (ASGR) were all expressed in mature HLCs (Figure 2a and Supporting Information Figure S5). The average of the ALB-positive cells in M1 to M5 was 9.8%, 16.6%, 20.8%, 37.7%, and 31.5%, respectively, and the percentage in M4 was significantly higher than in M1, M2, and M3, but not in M5 (Figure 2b). More than 90% of M2- to M5-HLCs were positive for ASGR (data not shown).

3.3 | Gene regulation

As expected, *OCT4* was highly expressed at the iPSC stage, whereas at the DE stage, *OCT4* was dramatically downregulated in most of the cell lines, and *SOX17* and *FOXA2* were highly expressed (Supporting Infomation Figure S6). Further differentiation toward HLCs resulted in significant downregulation of *SOX17*, whereas *FOXA2* remained upregulated during the rest of the differentiation and maturation of the HLCs (Figure 2c and Supporting Infomation Figure S7). The HLCs expressed *SOX17* at the same levels as hLTR. The level of *FOXA2* in the HLCs was comparable to those in the reference samples PHH, hLTR, and HepG2. *AFP* was upregulated during the early and late hepatic differentiation stages, indicating the immature characteristic of the HLCs. The expression of *AFP* in the M2-HLCs was statistically significantly higher than in the M1-HLCs. *ALB* was dramatically upregulated in mature HLCs, up to 2×10^5-fold compared with that in the hiPSCs, and its levels remained close but below those found in the PHHs. The expression of *ALB* in the M5-HLCs was significantly higher than in the M1-HLCs ($p < 0.01$) and M3-HLCs ($p < 0.05$). The levels of *ALB* expression were comparable between the HepG2 and the PHHs; however, *ALB* expression was about 19-fold higher in the hLTR when compared with the PHHs.

3.4 | Hepatic maturation and functionality

The liver is responsible for producing serum albumin. Therefore, we evaluated the ability of HLCs to secrete albumin into the conditioned medium. All HLCs were able to secrete albumin (Figure 2d). Albumin secretion by UTA.11304 differentiated by M3 was about fourfold
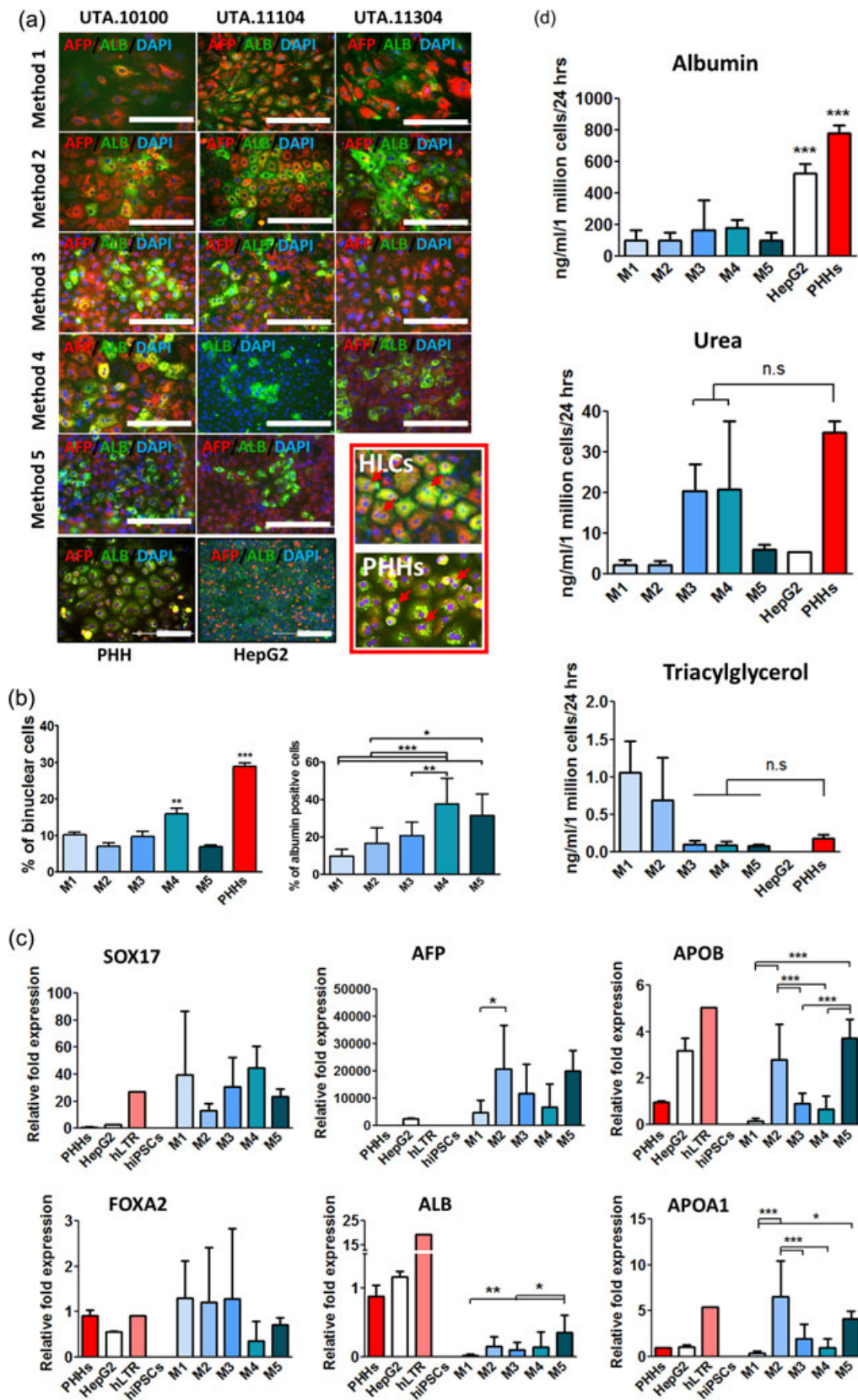
FIGURE 2 Continued.

higher compared with the same cell line differentiated by M1 or M2, and twofold higher compared with M4 (data not shown), but no other statistically significant differences were observed between the differentiation protocols. However, PHHs secreted significantly larger amounts of albumin than the HLCs or even the HepG2 cells.

The level of secreted urea by the cell lines differentiated by M3 and M4 was considerably higher compared with same lines differentiated by M1, M2, and M5 and relatively closer to the amount of urea secreted by the PHHs (Figure 2d). In fact, the level of urea secreted by the HLCs differentiated by M1, M2, and M5 was comparable to the HepG2 cells, which secreted 6.5-fold less urea than the PHHs.

TAG secretion in the cell lines differentiated by M3, M4, and M5 was at similar levels as in the PHHs (Figure 2d). However, cell lines differentiated by M1 and M2 secreted, on average, 5.9- and 3.8-fold more TAG than the PHHs. We were not able to detect secreted TAG in the HepG2 culture medium due to medium interference.

Apolipoprotein A-I (*APOA1*) encodes for apoA, which is the main protein component of high-density lipoproteins (HDL). The product of apolipoprotein B (*APOB*) is the main protein component of very-low-density lipoprotein (VLDL) and LDL. The expression of both *APOA1* and *APOB* in the HLCs was comparable to the HepG2 cells, PHHs, and hLTR, which further indicated the functionality of the HLCs (Figure 2c). Interestingly, both *APOA1* and *APOB* were expressed almost 5.5-fold more in hLTR compared with the PHHs.

All the cell lines were able to uptake the labeled LDL from the culture medium (Supporting Information Figure S5). This was confirmed by staining the LDL-R by monoclonal antibody (Supporting Information Figure S4).

3.5 | Lipid profiles of HLCs differentiated by different methods

The HLCs differentiated by M3, M4, and M5 showed superior functionality as for TAG and urea secretion when compared with M1 and M2. In addition, the M5-HLCs expressed higher *ALB* compared with the HLCs differentiated by M1 and M3. Therefore, we selected the HLCs differentiated by M3, M4, and M5, analyzed their lipid profile by MS, and compared their lipid profile. In addition, the lipid contents of their unconditioned media were studied to investigate the influence of culture media lipids and their FAs on the cells.

Overall, 15 major lipid classes—including CE, DAG, PC, LPC, PI, LPI, PE, LPE, SM, Cer, LacCer, Glc/GalCer, and Gb3—were investigated, and altogether more than 150 molecular species were detected and studied (Supporting Information Tables S2 and S3).

The lipid profile of the HLCs differentiated by M3, M4, and M5 closely resembled each other (Figures). In fact, only the levels of three PC species (PC 16:1–20:4, PC 17:0–18:1, and PC 17:0–20:4) were slightly, but statistically significantly, lower in M4 (Figure 3, marked by blue arrows) compared with the other methods. No other significant differences were found in any of the molecular species between the methods. When comparing the total levels of lipid classes, only Cer was found at significantly lower concentrations in the cells produced by M5 compared with those produced by M4 (Figure 5b). However, at the molecular species level, none of the Cer species differed significantly between M4 and M5 (Figure 5a and Supporting Information Table S2).

3.6 | Lipid profiles of HLCs, PHHs, and HepG2 cells

Next, we compare the lipidomes of the HLCs with the PHHs and HepG2 cells and describe our findings for each lipid class separately. In addition, we highlight the differences and similarities between the PHHs and HepG2 cells.

3.6.1 | Phospholipids

In the HLCs, the molecular species of PC, PE, and PI containing saturated FAs (SFAs) and monounsaturated FAs (MUFAs) were mostly similar to those in the PHHs, with the exceptions of PC 18:1/18:1 ($p < 0.05$), PC 17:0–18:1 ($p < 0.001$), and PE 18:0–18:1 ($p < 0.05$), which were statistically significantly higher in the HLCs (Figure 3, marked by red arrows). When the PHHs were compared with the HepG2 cells, a large number of species showed statistically significant differences, particularly the species containing 14:0, 16:0, and 18:1 FAs. In PC and PE, the molecular species containing polyunsaturated FAs (PUFAs) were present in significantly higher concentrations in the PHHs compared with both the HLCs and HepG2 cells. This difference was especially pronounced for the species containing an SFA coupled with FA 18:2 or its derivative 20:4 (e.g., 16:0–18:2, 18:0–18:2, 16:0–18:2, and 18:0–20:4). The HepG2 cells, however, contained more of the species where an MUFA was

FIGURE 2 Characterization and functionality of hiPSC-derived hepatocyte-like cells (hiPSC-HLCs) differentiated from three cell lines by five methods and their comparison to primary human hepatocytes (PHHs), HepG2 cells, and human liver total RNA (hLTR). (a) Immunostaining of cells for AFP (red) and ALB (green). Nuclei are stained with DAPI (blue). The red inset on the lower right shows the comparison of the morphology and binuclearity (red arrows) of M5-HLCs and PHHs. The scale bar represents 200 μm for the HLCs and 100 μm for the PHHs and HepG2 cells. (b) The graph on the left shows the average percentage of binuclear HLCs in each method and their comparison to PHHs. The graph on the right shows the average percentage of ALB-positive HLCs in each method. Each bar represents the mean ± SD of the manual counts from the immunostaining image analysis of at least five areas. (c) Real-time qPCR analysis of the *SOX17*, *FOXA2*, *AFP*, *ALB*, *APOA1*, and *APOB* genes at the hiPSC and hepatic stage and their comparison to the reference samples. Each sample was run in triplicate and the bars represent the mean ± SD of three biological replicates from three individual cell lines. The gene expression data were normalized to the housekeeping gene *GAPDH* and are presented relative to the PHHs. (d) Biochemical analysis of the conditioned media from the HLCs for albumin, urea, and triacylglycerol. Values are normalized as 1 million cells per 24 hr. The bars represent the mean ± SD of three biological replicates of the three cell lines. *$p < 0.05$, **$p < 0.01$, ***$p < 0.001$. DAPI: 6-diamidino-2-phenylindole; n.s.: not significant; qPCR: quantitative PCR; SD: standard deviation [Color figure can be viewed at wileyonlinelibrary.com]
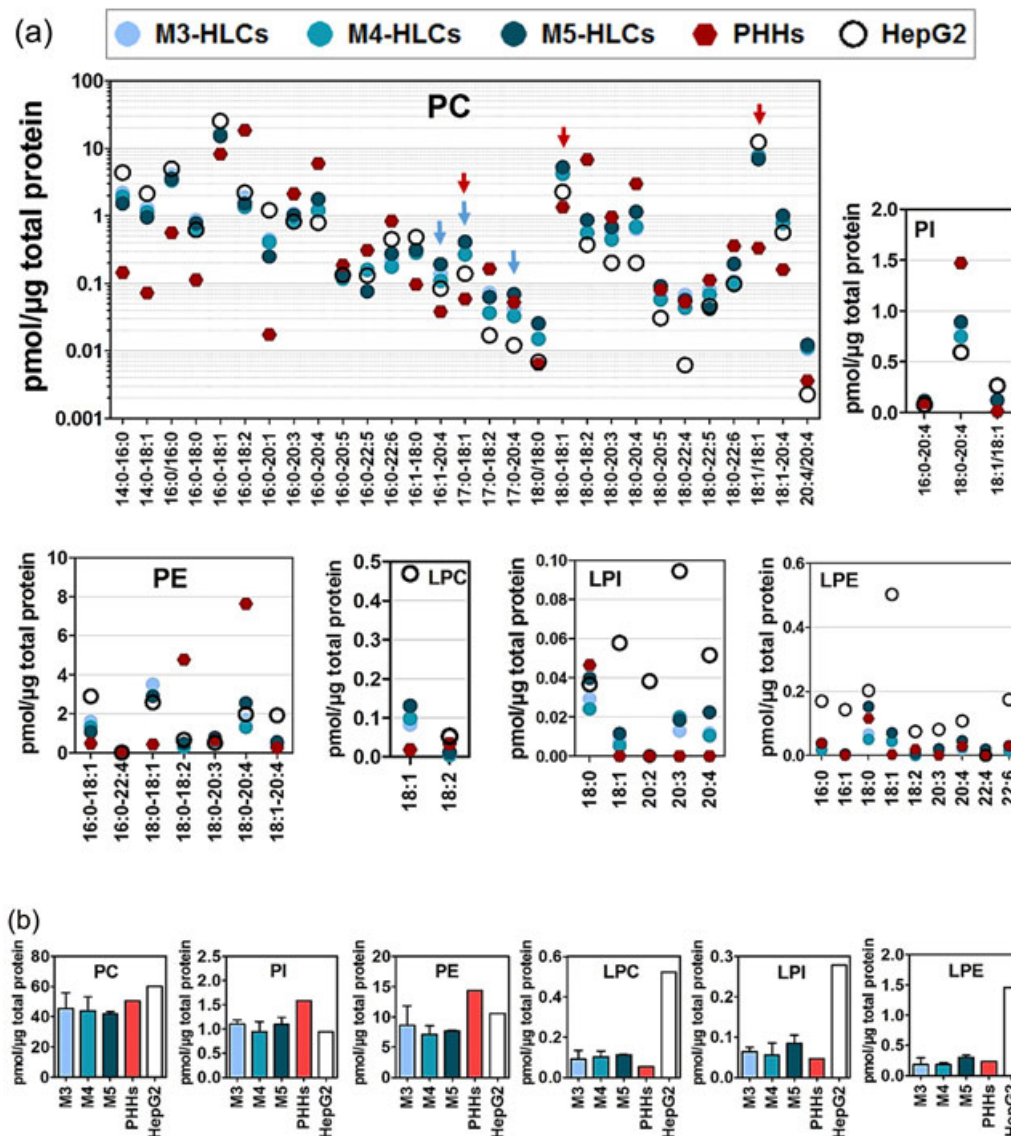
FIGURE 3 Lipidomic analysis of phospholipids (PLs) and lysophospholipids (LPLs) in the HLCs differentiated by M3, M4, and M5, and their comparison to PHH and HepG2 cell lipids. (a) Protein-normalized concentration of molecular species detected in each class of PLs (Phosphatidylcholine [PC], phosphatidylinositol [PI], and phosphatidylethanolamine [PE]) as well as LPLs (lysophosphatidylcholine [LPC], lysophosphatidylinositol [LPI], and lysophosphatidylethanolamine [LPE]). The arrows refer to species that were found to be statistically significantly different between HLCs in M3, M4, and M5 (blue arrows) or between the HLCs and PHHs (red arrows) by one-way analysis of variance. (b) Total concentrations of PLs and LPLs calculated from the sum of all the molecular species in those specific classes. Each sample was run in triplicate and the bars represent the mean ± standard deviation of the studied cell lines [Color figure can be viewed at wileyonlinelibrary.com]

coupled to a PUFA (or another MUFA). The total levels of PC and PI classes were similar among all three compared cell types. Total PE was, however, detected at lower levels in the HLCs compared with the PHHs (statistically significant in M4 and M5 vs the PHHs). This was mostly due to the higher levels of PE 18:0–18:2 and PE 18:0–20:4 in the PHHs. The concentration of PC, PE, and PI in the HLC and PHH media was either zero or negligible, while the HepG2 medium contained high amounts of PC (12.9 μM) but only minimal amounts of PE and PI (Supporting Information Figure S7 and Table S3). The profile and concentration of molecular lysophospholipids (LPLs)—such as LPC, LPE, and LPI—in the HLCs were very close to those of the PHHs (Figure 3a). Consequently, the total LPL levels of the HLCs

and PHHs were also similar (Figure 3b). The HepG2 cells, however, contained considerably higher levels of LPL as total levels and strikingly high levels of the molecular lyso-species, with the 18:1 acyl residue in each LPL class (Figure 3 and Supporting Information Table S2).

3.6.2 | Neutral lipids

CE concentration was the highest in the HepG2 cells, intermediate in the HLCs, and the lowest in the PHHs. The CE species profile of the HLCs and HepG2 cells was different because 16 CE species showed statistically significantly higher concentrations in the HepG2 cells
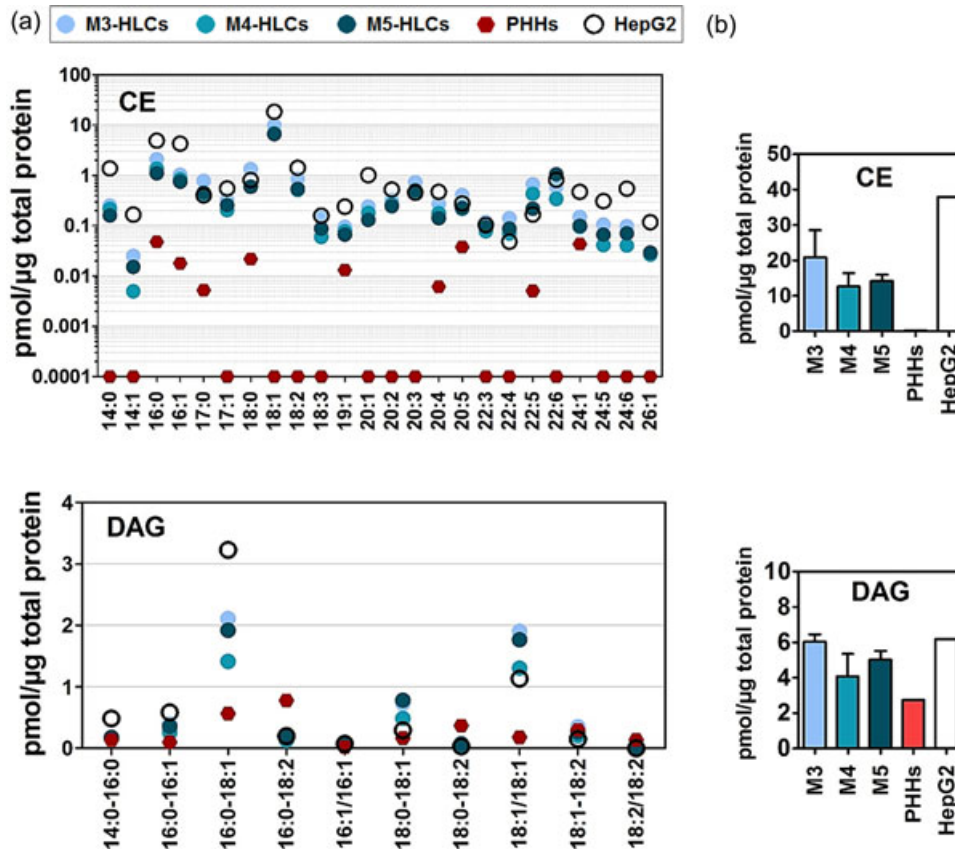
FIGURE 4 Lipidomic analysis of cholesteryl ester (CE) and diacylglycerol (DAG) in the HLCs differentiated by M3, M4, and M5, and their comparison to PHH and HepG2 cell lipids. (a) Protein-normalized concentration of molecular species detected for the CE and DAG lipid class. (b) Total concentrations of CE and DAG calculated from the sum of all the molecular species in those specific classes. Each sample was run in triplicate and the bars represent the mean ± standard deviation of the studied cell lines [Color figure can be viewed at wileyonlinelibrary.com]

(Figure 4). When interpreting these differences, the effect of medium CE concentration was considered. The HepG2 medium contained 154 μM of CE, whereas the CE concentrations were negligible in the HLC and PHH media (Supporting Information Figure S7 and Table S3).

Similar to PLs, the HLCs contained higher levels of DAG species with FA 18:1 when compared with the PHHs. However, the level of major DAG species 16:0–18:1 detected in the HLCs was clearly closer to that detected in the PHHs compared with what was found in the HepG2 cells. The PHHs, on the other hand, contained higher levels of DAG species with FA 18:2 (the minor species DAG 18:1–18:2 being an exception with its equally low levels in the HLCs, PHHs, and HepG2 cells). As also observed in PC, the DAG species with relatively short chain FAs (e.g., 14:0, 16:0, and 16:1) were detected at higher concentrations in the HepG2 cells than in the HLCs and PHHs (Figure 4A).
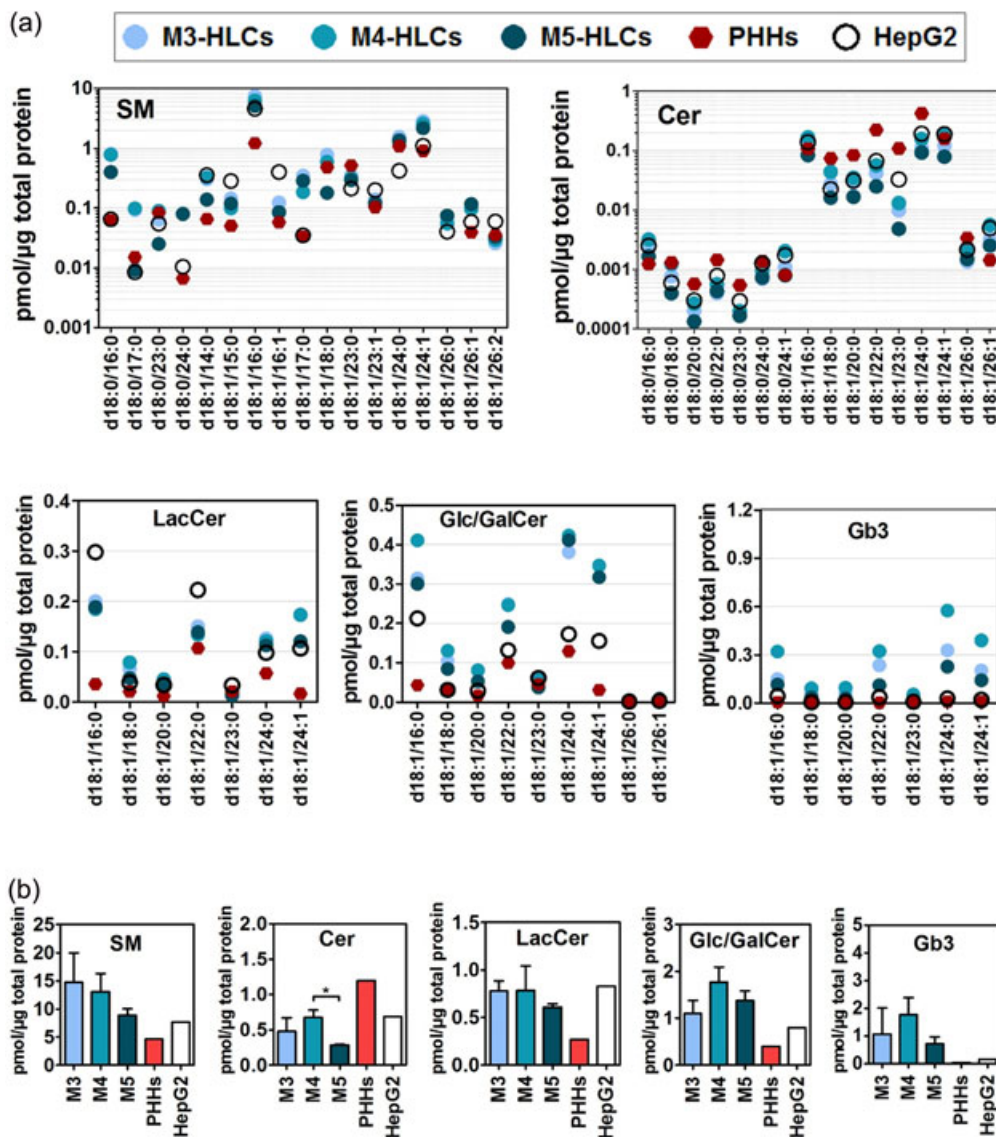
3.6.3 | Sphingolipids

Despite higher total SM concentration, HLCs mimicked the SM profile of PHHs and HepG2 cells, except that SM d18:1/15:0 and SM d18:1/16:1 were present at statistically significantly higher concentrations in the HepG2 cells (Figure 5a). Both the HLCs and HepG2 cells contained significantly higher levels of SM d18:1/16:0 compared

with the PHHs. The level of SM in the HLC and PHH media was undetectable, whereas the HepG2 medium contained 6.5 μM of SM (Supporting Information Figure S7 and Table S3).

In terms of the overall SL profile, the HepG2 cells situated between the PHHs and HLCs. In fact, lipid class data showed that the HLCs contained lower levels of Cer but higher levels of LacCer, Glc/GalCer, and Gb3 (members of glycosphingolipid [GSL] family) compared with the PHHs (Figure 5b). Closer examination showed that Cers and, particularly, the saturated species with long- and very-long-chain FAs (e.g., Cer d18:0/22:0 and Cer d18:1/24:0) were higher in the PHHs (Figure 5a), in fact, the Cer species profile of the HLCs resembled more that of the HepG2 cells. On the other hand, the HLCs contained more GSLs—especially the species d18:1/16:0, d18:1/24:0, and d18:1/24:1—and the differences were the most pronounced in the Glc/GalCer class. The HepG2 medium contained trace amounts of SLs, and the concentration of SLs in the HLC and PHH media was either negligible or undetectable (Supporting Information Figure S7 and Table S3).

3.7 | FA analysis

The HLCs contained 15 mol% PUFAs versus 29 mol% and 10.5 mol % in the PHHs and HepG2 cells, respectively (Figure 6a). The FA

FIGURE 5 Lipidomic analysis of sphingolipids (SLs) in the HLCs differentiated by M3, M4, and M5, and their comparison to the PHHs and HepG2 cells. (a) Protein-normalized concentration of molecular species detected for the sphingomyelin (SM), ceramide (Cer), glucosyl/galactosylceramide (Glc/GalCer), lactosylceramide (LacCer), and globotriaosylceramide (Gb3) lipid classes. (b) Total concentrations of SLs calculated from the sum of all the molecular species in those specific classes. Each sample was run in triplicate and the bars represent the mean ± standard deviation of the studied cell lines. *$p \leq 0.05$ [Color figure can be viewed at wileyonlinelibrary.com]

18:2n-6 was, in proportion, the highest PUFA detected in the PHHs (14 mol%); it was also the highest PUFA detected in the PHH medium (89 mol%; Figure 6b and Supporting Information Table S3). Both the HLCs and HepG2 cells had a low supply of 18:2n-6 in their media and, hence, lower relative levels of 18:2n-6 in their cellular FA profile. Interestingly, the HLCs seemed to be able to compensate for the shortage of supply better than the HepG2 cells, and the levels of 20:4n-6, a bioactive metabolite of 18:2n-6, were only 1.4-fold lower in the HLCs compared with the PHHs, indicating an active biosynthesis of 20:4n-6 from its precursor in the HLCs.

The total levels of MUFAs in the HLCs (43 mol%) were higher than in the PHHs (25 mol%), but they were still lower than in the HepG2 cells (52 mol%) (Figure 6a). FA 18:1n-9 (with its 31 mol% of all

FAs) was the major MUFA in the HLCs, a reflection of the high concentration of 18:1n-9 in their medium. FA 16:1n-7 (an SCD Δ9-desaturation product of 16:0) had the lowest values in the HLCs (0.6-fold the PHH level) and the highest values in the HepG2 cells (1.4-fold the PHH level). Consequently, the relative concentration of 18:1n-7 (an fatty acid elongase (ELOVL)5/6 chain elongation product of 16:1n-7) was the highest in the HepG2 cells (14 mol%) and lower in HLCs and PHHs (4 mol% and 2 mol%, respectively). This implies that the high 18:1n-7 is a specific feature of HepG2 cells, marking a clear distinction from the HLCs and PHHs, which appeared similar in having 18:1n-9 as their main MUFA component.

The total SFAs in the HLCs, PHHs, and HepG2 cells were 40 mol %, 46 mol%, and 37 mol%, respectively (Figure 6a). Relative to the PHHs, the lower SFAs in the HLCs were attributable to the slightly
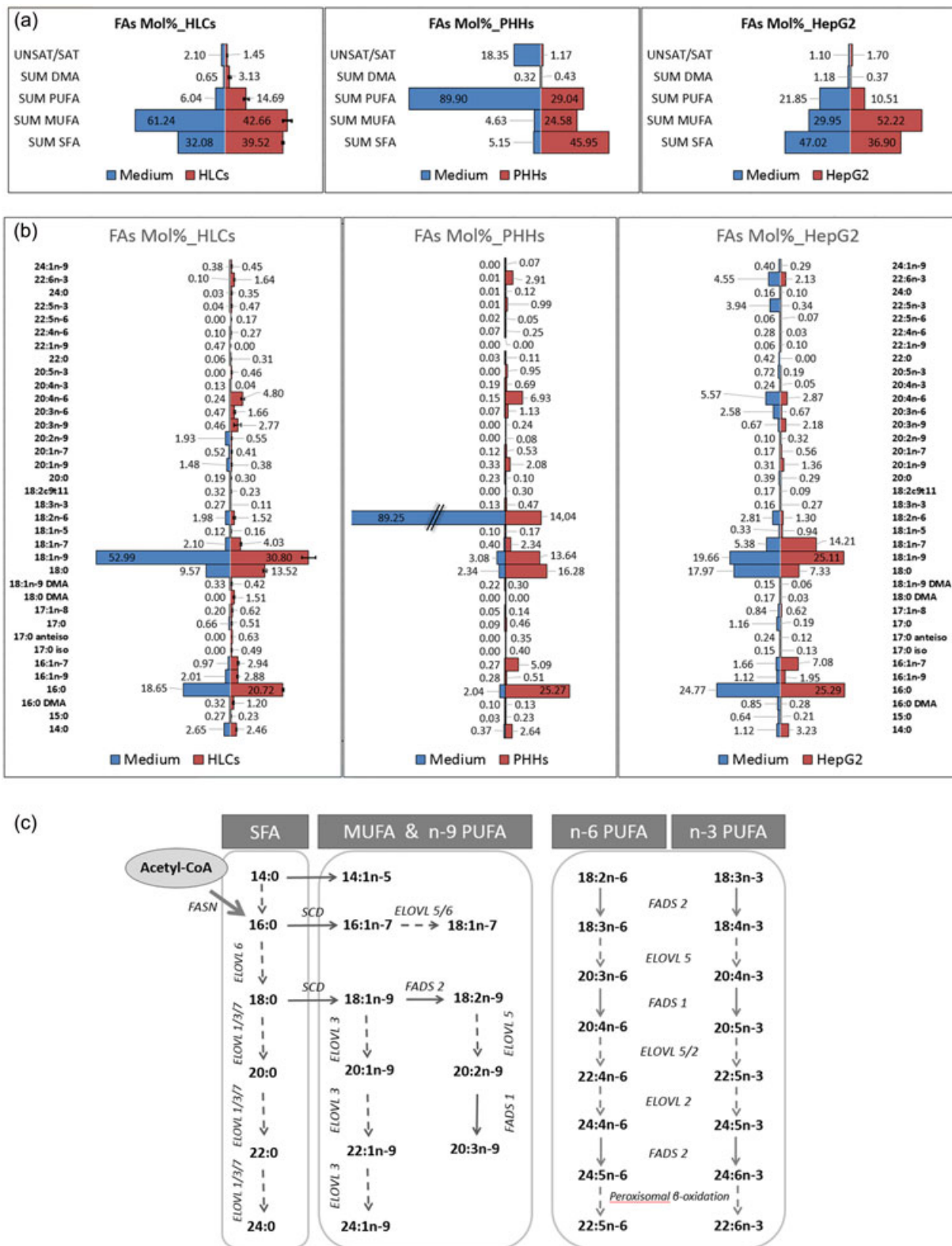
FIGURE 6 Fatty acid (FA) analysis (mole% in total FAs) of the M3-HLCs, PHHs, and HepG2 cells versus their media. (a) Total proportions of saturated fatty acids (SFAs), monounsaturated fatty acids (MUFAs), polyunsaturated fatty acids (PUFAs), and dimethyl acetals (DMAs, derived from plasmalogen PL alkenyl chains) in the studied cell types and their media. The ratio of total unsaturated FAs (UNFAs) to total SFAs is shown on the top bar. (b) Mirrored bar chart presenting the FA profiles in the M3-HLCs, PHHs, and HepG2 cells (red bars) in comparison to their media (blue bars). Each bar represents the mol% of the detected FAs. Error bars in the HLCs are calculated from the mean ± standard deviation of three biological replicates. (c) Schematic image of the metabolic pathways of SFAs, MUFAs, and PUFAs, including the responsible genes (*FASN, SCD, ELOVL, FADS*). The figure is adapted from the work by Glück et al., (2016). HLC: hepatocyte-like cell; PHH: primary human hepatocyte; PL: phospholipid [Color figure can be viewed at wileyonlinelibrary.com]

lower proportion of all major individual FAs (14:0, 16:0, and 18:0). The lower amount of total SFAs in the HepG2 cells, however, was mainly due to the considerably lower percentage of 18:0 compared with the PHHs (2.2-fold less).

3.8 | Gene expression of key enzymes in FA metabolism

To further investigate the metabolism of FAs in the HLCs, PHHs, and HepG2 cells, we studied the expression of five key genes involved in the synthesis pathways of FA by qPCR. Lipogenesis is highly affected by glucose homeostasis in the liver. Therefore, the expression of Glucokinase (encoded by *GCK*), the key enzyme involved in glycolysis, was also studied. The results revealed that FA synthase (*FASN*), a key gene in de novo FA synthesis, was expressed in the HLCs mostly at similar levels as in the PHHs (Figure 7a). The *FASN* expression level of the HepG2 cells was higher than that of the PHHs. The expression of *GCK* in HLCs was at similar levels as in

the PHHs (Figure 7b). Comparing the methods, M3-HLCs and M4-HLCs expressed *GCK* at statistically significantly higher levels than M1-HLCs. FA desaturase 1 (*FADS1*) was expressed at a statistically significantly lower level in all the HLCs ($p < 0.001$) when compared with the PHHs, but at similar levels as in hLTR and the HepG2 cells. In the HepG2 cells, hLTR, and almost half of the HLCs, *FADS2* was expressed at lower levels than in the PHHs. In the other half of the studied HLCs, the expression of *FADS2* was similar to that in the PHHs (Figure 7a). In addition to the FADSs, FA elongases *ELOVL2* and *ELOVL5*, working in sequence with the desaturases, are essential for the metabolism of long-chain and highly unsaturated FAs (Figure 6c). *ELOVL2* was expressed in most of the HLC lines at similar levels to the PHHs, but some lines produced by M2, M3, and M5 showed statistically significantly higher expression levels (Figure 7a). The expression of *ELOVL2* was statistically significantly higher in the HepG2 cells than in the PHHs. *ELOVL5*, on the other hand, was expressed at roughly similar levels in all analyzed cells types (PHHs, HepG2 cells, hLTR, and HLCs).
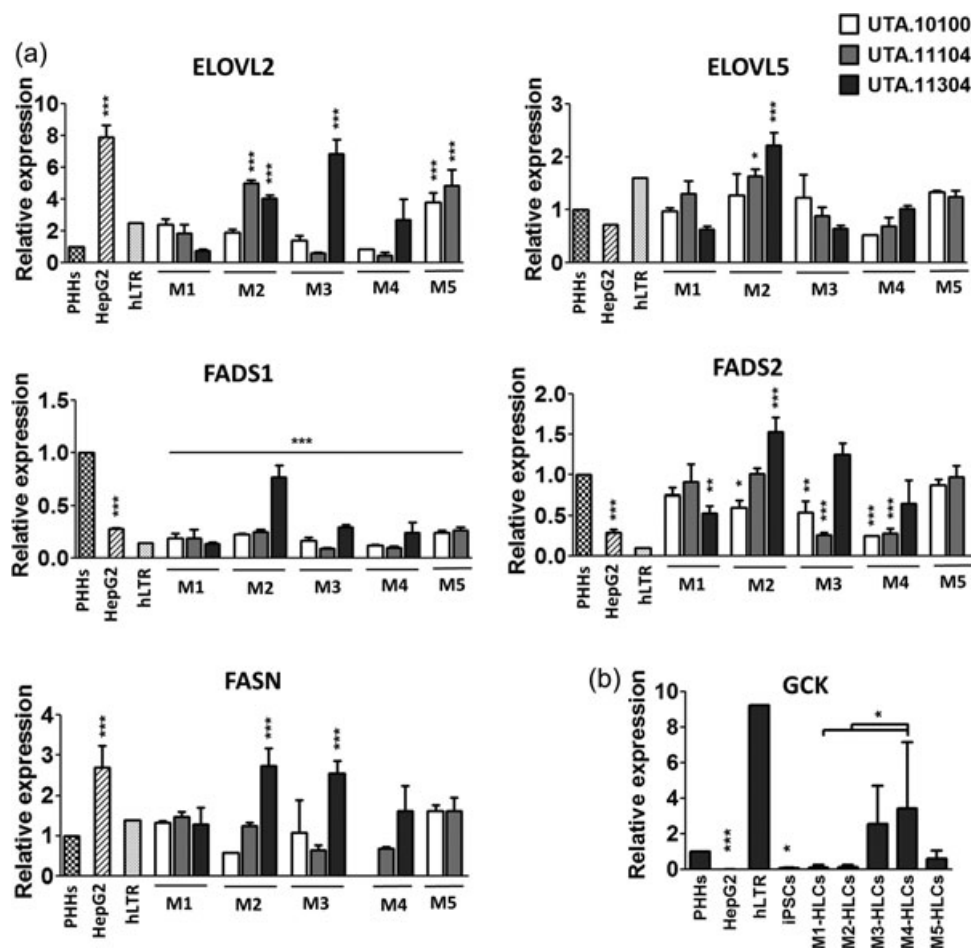
FIGURE 7 Expression levels of genes involved in the metabolism of fatty acids (FAs) (a) and glucose (b). (a) Real-time qPCR analysis of *ELOVL2*, *ELOVL5*, *FADS1*, *FADS2*, and *FASN* in the HLCs (differentiated by five methods), PHHs, HepG2 cells, and human liver total RNA (hLTR). (b) Real-time qPCR analysis of *GCK* in HLCs (differentiated by five methods), PHHs, HepG2 cells, hiPSCs, and human liver total RNA (hLTR). The expression of each gene was normalized to the endogenous control gene *GAPDH* and is presented relative to the PHHs. Each sample was run in triplicate, and the bars in the HLCs represent the mean ± standard deviation of three biological replicates. PHHs were used as reference group to calculate the statistical significance. *$p < 0.05$, **$p < 0.01$, ***$p < 0.001$. HLC: hepatocyte-like cell; PHH: primary human hepatocyte; qPCR: quantitative PCR

4 | DISCUSSION

hiPSC-HLCs are a promising cell culture platform for studying lipid homeostasis and its aberrations related to metabolic syndromes manifested, for example, in atherosclerosis and fatty liver disease. In the current study, we successfully generated functional HLCs from hiPSCs using five hepatic differentiation protocols. We then compared these HLCs comprehensively for gene and protein expression, lipid composition, and functional traits. Similar comparisons were also made with the two common hepatic cell models, PHHs and HepG2 cells. All five differentiation protocols produced HLCs capable of expressing *ALB*, uptaking LDL, and secreting albumin, urea, and TAG. The lipid profiles of the HLCs, PHHs, and HepG2 cells were analyzed by both MS and gas chromatography. In addition, the effects of FA supply from the culture media on the cells' lipid profile were examined. In this study, we performed, to our knowledge, the most thorough characterization of the metabolic traits of HLCs and investigated their potential as a new cell model for lipid studies in parallel with PHHs and HepG2 cells.

4.1 | Hepatic differentiation

Most protocols for differentiating HLCs from pluripotent stem cells follow a three-step differentiation through the DE phase, continuing to the hepatoblast stage, and finally to mature HLCs. Various growth factors and cytokines known to be necessary for liver development are used through these procedures (Cameron et al., 2015; Chen et al., 2012; Gerbal-Chaloin et al., 2014; Hannan et al., 2013; Hu & Li, 2015; Mallanna & Duncan, 2013; Schwartz, Fleming, Khetani, & Bhatia, 2014; Si-Tayeb et al., 2010; Sullivan et al., 2010; Takayama et al., 2012). We observed that at the DE stage, the initial density of the hiPSCs played a more critical role than the type of DE inducer (e.g., CHIR 99021 or Wnt3). In fact, high initial cell density in M1, M2, and M5 leads to remaining undifferentiated colonies, whereas in M3 and M4, this results in the formation of new dense and undifferentiated areas. On the other hand, very low initial cell density could lead to highly sparse cells and consequently unsuccessful differentiation. Hence, it is fundamental to find the optimal cell density for each cell line in each method.

At the hepatoblast stage, cells in M1 were supplemented with FGF2 and BMP4, mimicking the stimuli present during liver development (Rasmussen, 2015). However, in other methods, DMSO was used instead of FGF2 and BMP4. DMSO has histone deacetylase inhibitor activity and significantly increases the expression levels of BMP2 and BMP4 while decreasing the expression levels of stem cell markers, such as Oct4 (Behbahan et al., 2011; Choi et al., 2015; Czysz, Minger, & Thomas, 2015; Santos, Figueira-Coelho, Martins-Silva, & Saldanha, 2003). At Day 10, the cells in M1 had clear borders; they had also formed sinusoidal canaliculi-like structures (Supporting Information Figure S1b). However, at the end of the hepatoblast stage and the beginning of the maturation stage, the cells in M2, M3, M4, and M5 also eventually gained sinusoidal canaliculi-like structures (Supporting Information Figure S3). In addition, small lipid droplets were clearly visible in the cells in the culture medium containing DMSO, which could be due to excess of FA supplies in that medium (Kiamehr et al., 2017).

For the maturation of hepatocytes, HGF and oncostatin M were used. Epidermal growth factor (EGF) was present only in M3, M4, and M5. It has been shown that HGF and EGF—two tyrosine kinase receptor ligands—together decrease the expression of several genes involved in the metabolism of FAs (Michalopoulos, Bowen, Mulè, & Luo, 2003). In our study, EGF seemed to affect urea and TAG secretion but not the albumin secretion of the HLCs. In fact, M3-, M4-, and M5-HLCs secreted both urea and TAG similarly to the PHHs, but clearly different from the levels secreted by the M1- and M2-HLCs (Figure 2D).

It has been proposed that the unnatural microenvironment provided by current culture systems is partly responsible for the immature features of HLCs (Godoy et al., 2015), and that coating the culture plates with a mixture of Laminin 521/111 could further promote HLC maturation (Cameron et al., 2015). Hence, in M4 we replaced the Geltrex coating with Laminin 521/111. Even though we did not observe this coating to improve functionality, it increased the number of ALB-positive cells by 82% and the binuclearity of HLCs by 65% compared with those in M3. In the adult liver, 15%–30% of hepatocytes are binuclear, and binucleation is usually considered a sign of terminal differentiation in hepatocytes, even though binuclear hepatocytes are still able to divide (Miyaoka & Miyajima, 2013). One study suggested that polyploid cells are more resistant to stressful conditions (Anatskaya & Vinogradov, 2007). However, the effect of size and number of nuclei on the hepatocyte function is an intriguing question yet to be answered.

It is well established that the levels of lipoproteins in the serum have a clear correlation with the risk of atherosclerosis (Moss, 1991). It has been shown that HLCs produce, secrete, and uptake cholesterol in vitro and that they robustly express apoprotein genes, for example, *APOA1*, *APOA2*, *APOB*, *APOC*, and *APOE* (Rasmussen, 2015). HLCs also respond to statin treatment in vitro by reducing the amount of secreted cholesterol (Krueger et al., 2013). Here, we confirmed that HLCs are capable of uptaking labeled LDL (Supporting Information Figure S5) as well as expressing *APOA1* and *APOB* at similar levels compared with PHHs (Figure 2c), which is in line with findings in other studies (Godoy et al., 2015). *APOA1* and *APOB* gene expression levels were studied as a surrogate for estimating the HDL and LDL production levels of HLCs.

Overall, the HLCs differentiated by M3, M4, and M5 showed superior characteristics for studying the liver function and lipid metabolism compared with the HLCs differentiated by M1 and M2. The M3-, M4-, and M5-HLCs secreted TAG at similar levels as the PHHs. In addition, the M3- and M4-HLCs secreted urea at levels closer to the PHHs when compared with the HLCs differentiated by other methods. M4 and M5 produced the most albumin-positive HLCs, and the M4-HLCs showed the highest binuclearity compared with the HLCs differentiated by the other methods. Furthermore, we observed that the cell lines differentiated by M5 showed the least variation. This could be attributed to the application of the STEMdiff™ DE kit at the DE stage, which resulted in uniform DE differentiation. Because the DE stage is the key phase in hepatic differentiation, evenly differentiated

DE cells could result in more uniform hepatic differentiation, reducing possible variation between cell lines. Nevertheless, it should be considered that the Laminin coating applied in M4 and the STEMdiff™ DE kit used in M5 adds to the overall costs of the differentiation and makes these methods more expensive than, for example, M3.

4.2 | Lipid profiling

PUFAs and their bioactive derivatives play important roles during cell proliferation and differentiation (Bieberich, 2012; Kim, Kim, Kim, Kim, & Han, 2009). It has previously been shown that the addition of certain FAs, such as docosahexaenoic acid (22:6 n-3) or eicosapentaenoic acid (20:5 n-3), to the media could promote neuronal differentiation in neuronal stem/progenitor cells through the regulation of the cell cycle (Katakura et al., 2013). Furthermore, a definite mixture of FAs induces adipocyte-like differentiation of osteosarcoma cells through the activation of peroxisome proliferator-activated receptors (Diascro et al., 1998). It is known that the endogenous capacity of cultured cells to modify PUFAs for their needs can partially compensate for suboptimal supply from the microenvironment and culture medium (Zhang, Kothapalli, & Brenna, 2016). A simplified schematic figure of the metabolic pathways of SFAs, MUFAs, and PUFAs and the genes involved is presented in Figure 6c. PHHs possess an excellent capacity to metabolize diet-derived PUFAs (Sprecher, 2000). Most of our HLC lines expressed the key enzymes in the metabolism of FAs at similar levels to the PHHs. The HepG2 cells, however, varied significantly in most of the studied enzymes compared with the PHHs. This indicates that HLCs are superior cell models for studying the FA metabolism of the liver compared with HepG2 cells.

Our analysis revealed that PHHs contain a considerably larger proportion of PUFAs compared with HLCs and HepG2 cells. The high percentage of 18:2n-6 in the PHHs reflects the very rich supply of 18:2n-6 from the medium, part of which was apparently converted to 20:4n-6 by the cells using the FADS2, ELOVL5, and FADS1 enzymes. Even though the 18:2n-6 level in the HLCs medium was very low, these cells were able to efficiently produce 20:4n-6, suggesting the proper expression of FADS2, ELOV5, and FADS1. Interestingly, the main n-3 PUFA, 22:6n-3, was also detected in the HLCs with levels only 1.8-fold lower than in the PHHs, despite only trace amounts of n-3PUFAs in their medium. This result means that either the n-3PUFAs of HLCs originate from previous conditions (hepatoblast stage), or alternatively, these cells selectively and efficiently take up and incorporate 22:6n-3 into their lipids. The HepG2 cells received 22 mol% PUFAs from their medium, whereas the HLCs received only 6 mol%. In addition, the HepG2 medium was rich in the total FA content. Despite this, the relative levels of PUFAs in the HepG2 cells remained low (11 mol%) compared with the levels in the PHHs (29 mol%) and HLCs (15 mol%). The overloading of the HepG2 cells with the medium lipids and the consequent high content of neutral lipids (harboring fewer PUFAs than the structural PL) of the cells may have resulted in a relatively PUFA-poor FA composition in their total lipids.

In deficient states, endogenous synthesis of the 20:3n-9 from 18:1n-9 occurs (Kamada et al., 1999). It is of note that the HLCs and HepG2 cells both contained 2–3 mol% of n-9 PUFAs (20:2n-9 + 20:3n-9), which means that the cells suffered from essential PUFA deficiency. The large supply of 18:2n-6 in the PHH medium, however, prevented them from producing any significant amounts of n-9 PUFAs. PUFAs have been shown to be important in the maturation and functionality of HLCs (Kiamehr et al., 2017). Therefore, we propose that providing HLCs with a PUFA-rich medium may help to produce HLCs with a lipid profile even closer to PHHs. A high supply of PUFA to PHHs inhibits their endogenous MUFA synthesis from SFAs (Ntambi, 1999). Likewise, in our study, the total MUFA in the PHHs remained low compared to the HLCs and HepG2 cells. The lower the PUFA totals, the higher the MUFA totals were at the expense of the SFAs.

Hepatocytes can uptake FAs from the cell culture medium. Simultaneously, hepatocytes are able to produce FAs by hydrolyzing glucose to pyruvate, which links glycolysis to lipogenesis where pyruvate is used to synthesize FAs through de novo lipogenesis (Rui, 2014). Glucokinase (encoded by GCK gene) is central to the glucose homeostasis and is the key enzyme involved in the first step of glycolysis. Changes in hepatocyte GCK expression represent an adaptive action to impaired glucose/lipid metabolism to maintain glucose homeostasis (Massa, Gagliardino, & Francini, 2011). In our study, there were no significant differences in the expression of GCK between the HLCs and the PHHs. However, the HepG2 cells expressed GCK at statistically significantly lower levels than the PHHs, which is in line with previous findings at protein level (Wiśniewski, Vildhede, Norén, & Artursson, 2016). FASN is a major determinant of the capacity of a tissue to synthesize FAs de novo, and palmitate (16:0) is its primary product (Figure 6c; Jensen-Urstad & Semenkovich, 2012). Again, most HLC lines expressed FASN equally to the PHHs, whereas the HepG2 cells had clearly higher expression levels. The high expression of FASN in the HepG2 cells has also been observed earlier (Huang & Lin, 2012). The relative activities of SCD and ELOVL dictate whether the metabolism of 16:0 follows the route 16:0–16:1n-7–18:1n-7 or the route 16:0–18:0–18:1n-9 (Glück, Rupp, & Alter, 2016). In the former route, the SCD activity is higher than the ELOVL activity, and in the latter route, the ELOVL activity is higher than the SCD activity. Clearly, among the cells analyzed, the route forming 18:1n-7 was the most active in the HepG2 cells. This feature differentiates the HLCs and HepG2 cells and shows that the MUFA-producing pathway in HLCs resembles that found in PHHs. The elevated cellular contents of 16:1n-7 and high SCD activity appear to promote de novo lipogenesis, which could partially explain the large neutral lipid stores of the HepG2 cells (Hodson & Fielding, 2013).

4.3 | FAs mirrored in molecular species

We observed that the PL species profile of cells was highly affected by the culture medium. The PHHs' lipid profile reflected the high

medium supply of 18:2‐6, which after uptake was metabolized to 20:4n‐6 and incorporated into the PLs. Consequently, the PLs composed of 16:0–18:2, 18:0–18:2, 16:0–20:4, and 18:0–20:4 were abundant in the PHHs. The much lower supply of 18:2n‐6 to the HLCs and HepG2 cells kept the levels of the above-mentioned PL species low. However, the HLCs could still actively synthesize 20:4 and couple this PUFA with SFAs and MUFAs. To compensate for the overall PUFA deficiency, the HepG2 cells produced more MUFAs (observed in high levels of 18:1n‐7), which is reflected in species such as 16:0–18:1 and 18:1/18:1. The HLCs instead compensated for the PUFA shortage by uptaking 18:1n‐9, which was abundant in their medium.

In general, the HLCs and HepG2 cells contained lower concentrations of Cer and higher concentrations of LacCer, Glc/GalCer, and Gb3 when compared with the PHHs. Cer synthesis is a complex process orchestrated by six CerSs (CerS1–CerS6), each of which synthesizes Cers with distinct FA chain lengths (Cingolani, Futerman, & Casas, 2016). Cer has important structural and signaling roles (Gault, Obeid, & Hannun, 2010). It has been shown that at time of cellular stress, the generation of C16:0‐ceramide via CerS5 is proapoptotic, whereas synthesis of C24:0‐ceramides via CerS2 is prosurvival (Mesicek et al., 2010), and the balance between these long- and very-long-chain Cers is critical for cellular homeostasis. In our study, similar levels of d18:1/16:0 were observed in all three cell types, but the PHHs had significantly higher levels of d18:1/24:0 (Figure 5a). Transferring the PHHs from a physiological environment to an artificial 2D system could be stressful for them. Therefore, it is intriguing to speculate whether the survival or antiapoptosis mechanism is turned on in PHHs. On the other hand, HepG2 cells might suppress the apoptotic Cer signal by converting Cer to complex GSLs, leading to lowered levels of Cer in HepG2 cells. Overall, the interpretation of the observed Cer profile of the studied cell types is very complicated and demands further studies.

The UDP-glucose ceramide glucosyltransferase (*UGCG*) gene encodes the enzyme UDP-glucose Cer glucosyltransferase, which catalyzes the first glycosylation step in the biosynthesis of GSLs. The product of this reaction is glucosylceramide, which is the core structure of many GSLs, including Glc/GalCer (Tokuda et al., 2013). We have previously reported a higher expression of *UGCG* in HLCs compared with PHHs (Kiamehr et al., 2017), which correlates well with our lipidomics findings of high Glc/GalCer in HLCs. In the C24 species of every sphingolipid class, the ratio of the 24:0 species to the 24:1 species was higher in the PHHs than in the HLCs or HepG2 cells. This may reflect the dominance of 24:1n‐9 over 24:0 in both the HLC and HepG2 media and the reversed ratio of these trace MUFAs in the PHH medium.

The PHHs were cultured in a low FA medium. As a result, the PHHs contained low levels of CE in their cellular lipid profile. Unlike the PHH cells, the HepG2 cells—which were grown in FA-rich medium—accumulated a large amount of the neutral storage lipids CE and TAG, the latter being represented via its hydrolysis product DAG. As is normal for cultured cells, the highest CE species was 18:1, followed by 16:0 and 16:1, and there were also traces of various

other species. In line with the CE profile, the HepG2 cells contained large amounts of DAG, chiefly 16:0–18:1 and 18:1/18:1. The HLCs also showed an accumulation of neutral lipids (although milder than in the HepG2 cells), which is likely due to their treatment with an FA-rich medium at the hepatoblast stage (Day 6 to Day 12; Kiamehr et al., 2017). Therefore, our work reveals the need to revise the generally overlooked FA content of culture media and to tailor it according to the HLCs' needs. In addition, we propose that increasing the supply of PUFA in the culture medium may positively affect the lipid profile and functionality of the HLCs.

To our knowledge, this is the first comparative study that considers the effects of various stimuli from different protocols on the differentiation and phenotype of HLCs. We are also the first to show the detailed lipid profile of HLCs and to evaluate their ability to metabolize FAs. Taken together, HLCs differentiated from hiPSCs provide the advantage of direct studies of cellular and molecular mechanisms that regulate lipid homeostasis in the liver. They also facilitate a novel platform for the discovery, optimization, and study of the modes of action of molecules modulating key lipids. This platform would allow the functional assessment of the impact of genetic variations in developing metabolic diseases, such as atherosclerosis.

5 | CONCLUSIONS

HLCs mimicked the lipid profile of PHHs very well and, thus, showed to be a better liver cell model than HepG2 cells, especially in terms of their low LPL content. HLCs were capable of metabolizing FAs to produce C20–22 highly unsaturated FAs to fulfill the complex biological functions mediated by those FAs. By improving the PUFA supply in the medium, we can produce HLCs, which can serve as a powerful and functional cell model to study patient-specific mechanisms in lipid aberrations leading to pathological states, such as atherosclerosis or fatty liver disease.

The authors gratefully acknowledge the Tampere facility of iPS Cells and Flow Cytometry for their services.

ORCID

Mostafa Kiamehr http://orcid.org/0000-0003-1894-3237

REFERENCES

Anatskaya, O. V., & Vinogradov, A. E. (2007). Genome multiplication as adaptation to tissue survival: Evidence from gene expression in mammalian heart and liver. *Genomics*, 89(1), 70–80. http://doi.org/10.1016/j.ygeno.2006.08.014

Behbahan, I. S., Duan, Y., Lam, A., Khoobyari, S., Ma, X., Ahuja, T. P., & Zern, M. A. (2011). New approaches in the differentiation of human embryonic stem cells and induced pluripotent stem cells toward hepatocytes. *Stem Cell Reviews*, 7(3), 748–759. https://doi.org/10.1007/s12015-010-9216-4

Bieberich, E. (2012). It's a lipid's world: Bioactive lipid metabolism and signaling in neural stem cell differentiation. *Neurochemical Research*, 37, 1208–1229. https://doi.org/10.1007/s11064-011-0698-5

Blouin, A., Bolender, R. P., & Weibel, E. R. (1977). Distribution of organelles and membranes between hepatocytes and nonhepatocytes in the rat liver parenchyma. A stereological study. *The Journal of Cell Biology*, 72(2), 441–455.

Cameron, K., Tan, R., Schmidt-Heck, W., Campos, G., Lyall, M. J., Wang, Y., … Hay, D. C. (2015). Recombinant laminins drive the differentiation and self-organization of hESC-derived hepatocytes. *Stem Cell Reports*, 5(6), 1250–1262.

Castell, J. V., Jover, R., Martínez-Jiménez, C. P., & Gómez-Lechón, M. J. (2006). Hepatocyte cell lines: Their use, scope and limitations in drug metabolism studies. *Expert Opinion on Drug Metabolism & Toxicology*, 2(2), 183–212. https://doi.org/10.1517/17425255.2.2.183

Cayo, M. A., Cai, J., Delaforest, A., Noto, F. K., Nagaoka, M., Clark, B. S., … Duncan, S. A. (2012). JD induced pluripotent stem cell-derived hepatocytes faithfully recapitulate the pathophysiology of familial hypercholesterolemia. *Hepatology*, 56(6), 2163–2171. https://doi.org/10.1002/hep.25871

Chen, Y. F., Tseng, C. Y., Wang, H. W., Kuo, H. C., Yang, V. W., & Lee, O. K. (2012). Rapid generation of mature hepatocyte-like cells from human induced pluripotent stem cells by an efficient three-step protocol. *Hepatology*, 55(4), 1193–1203. https://doi.org/10.1002/hep.24790

Choi, S. C., Choi, J. H., Cui, L. H., Seo, H. R., Kim, J. H., Park, C. Y., … Lim, D. S. (2015). Mixl1 and Flk1 are key players of Wnt/TGF-β signaling during DMSO-induced mesodermal specification in P19 cells. *Journal of Cellular Physiology*, 230(8), 1807–1821.

Cingolani, F., Futerman, A. H., & Casas, J. (2016). Ceramide synthases in biomedical research. *Chemistry and Physics of Lipids*, 197, 25–32. https://doi.org/10.1016/j.chemphyslip.2015.07.026

Czysz, K., Minger, S., & Thomas, N. (2015). DMSO efficiently down regulates pluripotency genes in human embryonic stem cells during definitive endoderm derivation and increases the proficiency of hepatic differentiation. *PLoS One*, 10(2), e0117689. https://doi.org/10.1371/journal.pone.0117689

Diascro, D. D., Vogel, R. L., Johnson, T. E., Witherup, K. M., Pitzenberger, S. M., Rutledge, S. J., … Schmidt, A. (1998). High fatty acid content in rabbit serum is responsible for the differentiation of osteoblasts into adipocyte-like cells. *Journal of Bone and Mineral Research*, 13(1), 96–106. https://doi.org/10.1359/jbmr.1998.13.1.96

Ejsing, C. S., Duchoslav, E., Sampaio, J., Simons, K., Bonner, R., Thiele, C., … Shevchenko, A. (2006). Automated identification and quantification of glycerophospholipid molecular species by multiple precursor ion scanning. *Analytical Chemistry*, 78(17), 6202–6214. https://doi.org/10.1021/ac060545x

Ekroos, K., Chernushevich, I. V., Simons, K., & Shevchenko, A. (2002). Quantitative profiling of phospholipids by multiple precursor ion scanning on a hybrid quadrupole time-of-flight mass spectrometer. *Analytical Chemistry*, 74(5), 941–949. https://doi.org/10.1021/ac015655c

Ekroos, K., Ejsing, C. S., Bahr, U., Karas, M., Simons, K., & Shevchenko, A. (2003). Charting molecular composition of phosphatidylcholines by fatty acid scanning and ion trap MS3 fragmentation. *The Journal of Lipid Research*, 44(11), 2181–2192. http://doi.org/10.1194/jlr.D300020-JLR200

Elaut, G., Henkens, T., Papeleu, P., Snykers, S., Vinken, M., Vanhaecke, T., & Rogiers, V. (2006). Molecular mechanisms underlying the dedifferentiation process of isolated hepatocytes and their cultures. *Current Drug Metabolism*, 7(6), 629–660. http://doi.org/10.2174/138920006778017759

Gault, C. R., Obeid, L. M., & Hannun, Y. A. (2010). An overview of sphingolipid metabolism: From synthesis to breakdown. *Advances in Experimental Medicine and Biology*, 1–23. https://doi.org/10.1007/978-1-4419-6741-1_1

Gerbal-Chaloin, S., Funakoshi, N., Caillaud, A., Gondeau, C., Champon, B., & Si-Tayeb, K. (2014). Human induced pluripotent stem cells in hepatology: Beyond the proof of concept. *The American Journal of Pathology*, 184(2), 332–347. https://doi.org/10.1016/j.ajpath.2013.09.026

Glück, T., Rupp, H., & Alter, P. (2016). Mechanisms increasing n-3 highly unsaturated fatty acids in the heart. *Canadian Journal of Physiology and Pharmacology*, 94(3), 309–323. https://doi.org/10.1139/cjpp-2015-0300

Godoy, P., Hewitt, N. J., Albrecht, U., Andersen, M. E., Ansari, N., Bhattacharya, S., … Hengstler, J. G. (2013). Recent advances in 2D and 3D in vitro systems using primary hepatocytes, alternative hepatocyte sources and non-parenchymal liver cells and their use in investigating mechanisms of hepatotoxicity, cell signaling and ADME. . *Archives of Toxicology*, 87, 1315–1530. https://doi.org/10.1007/s00204-013-1078-5

Godoy, P., Schmidt-Heck, W., Natarajan, K., Lucendo-Villarin, B., Szkolnicka, D., Asplund, A., … Hengstler, J. G. (2015). Gene networks and transcription factor motifs defining the differentiation of stem cells into hepatocyte-like cells. *Journal of Hepatology*, 63(4), 934–942. https://doi.org/10.1016/j.jhep.2015.05.013

Gordillo, M., Evans, T., & Gouon-Evans, V. (2015). Orchestrating liver development. *Development*, 142(12), 2094–2108. https://doi.org/10.1242/dev.114215

Hannan, N. R. F., Segeritz, C.-P., Touboul, T., & Vallier, L. (2013). Production of hepatocyte-like cells from human pluripotent stem cells. *Nature Protocols*, 8(2), 430–437.

Hay, D. C., Fletcher, J., Payne, C., Terrace, J. D., Gallagher, R. C. J., Snoeys, J., … Iredale, J. P. (2008). Highly efficient differentiation of hESCs to functional hepatic endoderm requires ActivinA and Wnt3a signaling. *Proceedings of the National Academy of Sciences*, 105(34), 12301–12306. https://doi.org/10.1073/pnas.0806522105

Heiskanen, L. A., Suoniemi, M., Ta, H. X., Tarasov, K., & Ekroos, K. (2013). Long-term performance and stability of molecular shotgun lipidomic analysis of human plasma samples. *Analytical Chemistry*, 85(18), 8757–8763. https://doi.org/10.1021/ac401857a

Hodson, L., & Fielding, B. A. (2013). Stearoyl-CoA desaturase: Rogue or innocent bystander? *Progress in Lipid Research*, 52, 15–42. https://doi.org/10.1016/j.plipres.2012.08.002

Hu, C., & Li, L. (2015). In vitro culture of isolated primary hepatocytes and stem cell-derived hepatocyte-like cells for liver regeneration. *Protein & Cell*, 6(8), 562–574. https://doi.org/10.1007/s13238-015-0180-2

Huang, H. -C., & Lin, J. -K. (2012). Pu-erh tea, green tea, and black tea suppresses hyperlipidemia, hyperleptinemia and fatty acid synthase through activating AMPK in rats fed a high-fructose diet. *Food & Function*, 3(2), 170–177. https://doi.org/10.1039/C1FO10157A

Jensen-Urstad, A. P. L., & Semenkovich, C. F. (2012). Fatty acid synthase and liver triglyceride metabolism: Housekeeper or messenger? *Biochimica et Biophysica Acta*, 1821, 747–753. https://doi.org/10.1016/j.bbalip.2011.09.017

Kajiwara, M., Aoi, T., Okita, K., Takahashi, R., Inoue, H., Takayama, N., … Yamanaka, S. (2012). Donor-dependent variations in hepatic differentiation from human-induced pluripotent stem cells. *Proceedings of the National Academy of Sciences*, 109(31), 12538–12543. https://doi.org/10.1073/pnas.1209979109

Kamada, N., Kawashima, H., Sakuradani, E., Akimoto, K., Ogawa, J., & Shimizu, S. (1999). Production of 8,11-cis-eicosadienoic acid by a delta 5 and delta 12 desaturase-defective mutant derived from the arachidonic acid-producing fungus Mortierella alpina 1S-4. *Journal of the American Oil Chemists Society*, 76(11), 1269–1274. https://doi.org/10.1007/S11746-999-0138-8

Katakura, M., Hashimoto, M., Okui, T., Shahdat, H. M., Matsuzaki, K., & Shido, O. (2013). Omega-3 polyunsaturated fatty acids enhance neuronal differentiation in cultured rat neural stem cells. *Stem Cells International*, 2013, 1–9. https://doi.org/10.1155/2013/490476

Kia, R., Sison, R. L. C., Heslop, J., Kitteringham, N. R., Hanley, N., Mills, J. S., … Goldring, C. E. P. (2012). Stem cell-derived hepatocytes as a predictive model for drug-induced liver injury: Are we there yet? *British Journal of Clinical Pharmacology*, 75(4), 885–896. https://doi.org/10.1111/j.1365-2125.2012.04360.x

Kiamehr, M., Viiri, L. E., Vihervaara, T., Koistinen, K. M., Hilvo, M., Ekroos, K., … Aalto-Setälä, K. (2017). Lipidomic profiling of patient-specific induced pluripotent stem cell-derived hepatocyte-like cells. *Disease Models & Mechanisms*, 030841. https://doi.org/10.1242/dmm.030841

Kim, M. H., Kim, M. O., Kim, Y. H., Kim, J. S., & Han, H. J. (2009). Linoleic acid induces mouse embryonic stem cell proliferation via Ca 2+/PKC, PI3K/Akt, and MAPKs. *Cellular Physiology and Biochemistry*, 23(1–3), 53–64. https://doi.org/10.1159/000204090

Krueger, W. H., Tanasijevic, B., Barber, V., Flamier, A., Gu, X., Manautou, J., & Rasmussen, T. P. (2013). Cholesterol-secreting and statin-responsive hepatocytes from human ES and iPS cells to model hepatic involvement in cardiovascular health. *PLoS One*, 8(7), e67296.

Kvilekval, K., Lin, J., Cheng, W., & Abumrad, N. (1994). Fatty acids as determinants of triglyceride and cholesteryl ester synthesis by isolated hepatocytes: Kinetics as a function of various fatty acids. *Journal of Lipid Research*, 35(10), 1786–1794.

Livak, K. J., & Schmittgen, T. D. (2001). Analysis of relative gene expression data using real-time quantitative PCR and the 2− ΔΔCT method. *Methods*, 25(4), 402–408.

Mallanna, S. K., & Duncan, S. A. (2013). Differentiation of hepatocytes from pluripotent stem cells. *Current Protocols in Stem Cell Biology*, 1 (Suppl.26), 1G.4.1–1G.4.13. https://doi.org/10.1002/9780470151808.sc01g04s26

Manzini, S., Viiri, L. E., Marttila, S., & Aalto-Setälä, K. (2015). A comparative view on easy to deploy non-integrating methods for patient-specific iPSC production. *Stem Cell Reviews and Reports*, 11(6), 900–908. https://doi.org/10.1007/s12015-015-9619-3

Massa, M. L., Gagliardino, J. J., & Francini, F. (2011). Liver glucokinase: An overview on the regulatorymechanisms of its activity. *IUBMB Life*, 63, 1–6. https://doi.org/10.1002/iub.411

Medine, C. N., Lucendo-Villarin, B., Storck, C., Wang, F., Szkolnicka, D., Khan, F., … Hay, D. C. (2013). Developing high-fidelity hepatotoxicity models from pluripotent stem cells. *Stem Cells Translational Medicine*, 2 (7), 505–509. https://doi.org/10.5966/sctm.2012-0138

Meikle, P. J., Wong, G., Tsorotes, D., Barlow, C. K., Weir, J. M., Christopher, M. J., … Kingwell, B. A. (2011). Plasma lipidomic analysis of stable and unstable coronary artery disease. *Arteriosclerosis, Thrombosis, and Vascular Biology*, 31(11), 2723–2732. https://doi.org/10.1161/ATVBAHA.111.234096

Merrill , A. H., Jr., Sullards, M. C., Allegood, J. C., Kelly, S., & Wang, E. (2005). Sphingolipidomics: High-throughput, structure-specific, and quantitative analysis of sphingolipids by liquid chromatography tandem mass spectrometry. *Methods*, 36(2), 207–224. https://doi.org/10.1016/j.ymeth.2005.01.009

Mesicek, J., Lee, H., Feldman, T., Jiang, X., Skobeleva, A., Berdyshev, E. V., … Kolesnick, R. (2010). Ceramide synthases 2, 5, and 6 confer distinct roles in radiation-induced apoptosis in HeLa cells. *Cellular Signalling*, 22(9), 1300–1307. https://doi.org/10.1016/j.cellsig.2010.04.006

Michalopoulos, G. K., Bowen, W. C., Mulè, K., & Luo, J. (2003). HGF-, EGF-, and dexamethasone-induced gene expression patterns during formation of tissue in hepatic organoid cultures. *Gene Expression*, 11(2), 55–75. https://doi.org/10.3727/000000003108748964

Miyaoka, Y., & Miyajima, A. (2013). To divide or not to divide: Revisiting liver regeneration. *Cell Division*, 8, 8. https://doi.org/10.1186/1747-1028-8-8

Moss, A. J. (1991). Cholesterol and atherosclerosis: Diagnosis and treatment. *Journal of the American Medical Association*, 266(20), 2910–2911.

Ntambi, J. M. (1999). Regulation of stearoyl-CoA desaturase by polyunsaturated fatty acids and cholesterol. *Journal of Lipid Research*, 40(9), 1549–1558. Retrieved from. http://www.ncbi.nlm.nih.gov/pubmed/10484602

Ohnuki, M., Takahashi, K., & Yamanaka, S. (2009). Generation and characterization of human induced pluripotent stem cells. In Schlaeger, T. (Ed.), *Current protocols in stem cell biology*. John Wiley & Sons, Inc. https://doi.org/10.1002/9780470151808

Olsavsky, K. M., Page, J. L., Johnson, M. C., Zarbl, H., Strom, S. C., & Omiecinski, C. J. (2007). Gene expression profiling and differentiation assessment in primary human hepatocyte cultures, established hepatoma cell lines, and human liver tissues. *Toxicology and Applied Pharmacology*, 222(1), 42–56. https://doi.org/10.1016/j.taap.2007.03.032

Rasmussen, T. P. (2015). Genomic medicine and lipid metabolism: LDL targets and stem cell research approaches, *Translational Cardiometabolic Genomic Medicine* (99–118). London UK: Academic Press. https://doi.org/10.1016/B978-0-12-799961-6.00005-6

Ruhanen, H., Nidhina Haridas, P. A., Eskelinen, E. L., Eriksson, O., Olkkonen, V. M., & Käkelä, R. (2017). Depletion of TM6SF2 disturbs membrane lipid composition and dynamics in HuH7 hepatoma cells. *Biochimica et Biophysica Acta*, 1862(7), 676–685. https://doi.org/10.1016/j.bbalip.2017.04.004

Rui, L. (2014). Energy metabolism in the liver. *Comprehensive Physiology*, 4 (1), 177–197. https://doi.org/10.1002/cphy.c130024

Santos, N. C., Figueira-Coelho, J., Martins-Silva, J., & Saldanha, C. (2003). Multidisciplinary utilization of dimethyl sulfoxide: Pharmacological, cellular, and molecular aspects. *Biochemical Pharmacology*, 65, 1035–1041. https://doi.org/10.1016/S0006-2952(03)00002-9

Schwartz, R. E., Fleming, H. E., Khetani, S. R., & Bhatia, S. N. (2014). Pluripotent stem cell-derived hepatocyte-like cells. *Biotechnology Advances*, 32, 504–513. https://doi.org/10.1016/j.biotechadv.2014.01.003

Schwartz, R. E., Trehan, K., Andrus, L., Sheahan, T. P., Ploss, A., Duncan, S. A., … Bhatia, S. N. (2012). Modeling hepatitis C virus infection using human induced pluripotent stem cells. *Proceedings of the National Academy of Sciences of the United States of America*, 109, 2544–2548. https://doi.org/10.1073/pnas.1121400109/-/DCSupplemental.www.pnas.org/cgi//10.1073/pnas.1121400109

Si-Tayeb, K., Noto, F. K., Nagaoka, M., Li, J., Battle, M. A., Duris, C., … Duncan, S. A. (2010). Highly efficient generation of human hepato-

cyte–like cells from induced pluripotent stem cells. *Hepatology*, *51*(1), 297–305.

Sprecher, H. (2000). Metabolism of highly unsaturated n-3 and n-6 fatty acids. *Biochimica et Biophysica Acta*, *1486*, 219–231. https://doi.org/10.1016/S1388-1981(00)00077-9

Stübiger, G., Aldover-Macasaet, E., Bicker, W., Sobal, G., Willfort-Ehringer, A., Pock, K., … Belgacem, O. (2012). Targeted profiling of atherogenic phospholipids in human plasma and lipoproteins of hyperlipidemic patients using MALDI-QIT-TOF-MS/MS. *Atherosclerosis*, *224*(1), 177–186. https://doi.org/10.1016/j.atherosclerosis.2012.06.010

Sullivan, G. J., Hay, D. C., Park, I. -H., Fletcher, J., Hannoun, Z., Payne, C. M., … Wilmut, I. (2010). Generation of functional human hepatic endoderm from human induced pluripotent stem cells. *Hepatology*, *51*(1), 329–335. https://doi.org/10.1002/hep.23335

Szkolnicka, D., Farnworth, S. L., Lucendo-Villarin, B., Storck, C., Zhou, W., Iredale, J. P., … Hay, D. C. (2014). Accurate prediction of drug-induced liver injury using stem cell-derived populations. *Stem Cells Translational Medicine*, *3*(2), 141–148. https://doi.org/10.5966/sctm.2013-0146

Szkolnicka, D., Lucendo-Villarin, B., Moore, J. K., Simpson, K. J., Forbes, S. J., & Hay, D. C. (2016). Reducing hepatocyte injury and necrosis in response to paracetamol using noncoding RNAs. *Stem Cells Translational Medicine*, *5*(6), 764–772. https://doi.org/10.5966/sctm.2015-0117

Takahashi, K., & Yamanaka, S. (2006). Induction of pluripotent stem cells from mouse embryonic and adult fibroblast cultures by defined factors. *Cell*, *126*(4), 663–676.

Takayama, K., Inamura, M., Kawabata, K., Sugawara, M., Kikuchi, K., Higuchi, M., … Mizuguchi, H. (2012). Generation of metabolically functioning hepatocytes from human pluripotent stem cells by FOXA2 and HNF1α transduction. *Journal of Hepatology*, *57*(3), 628–636. https://doi.org/10.1016/j.jhep.2012.04.038

Tokuda, N., Numata, S., Li, X., Nomura, T., Takizawa, M., Kondo, Y., … Furukawa, K. (2013). β4GalT6 is involved in the synthesis of lactosylceramide with less intensity than β4GalT5. *Glycobiology*, *23*(10), 1175–1183. https://doi.org/10.1093/glycob/cwt054

Wiśniewski, J. R., Vildhede, A., Norén, A., & Artursson, P. (2016). In-depth quantitative analysis and comparison of the human hepatocyte and hepatoma cell line HepG2 proteomes. *Journal of Proteomics*, *136*, 234–247. https://doi.org/10.1016/j.jprot.2016.01.016

Yang, D., Yuan, Q., Balakrishnan, A., Bantel, H., Klusmann, J., Manns, M. P., … Sharma, A. D. (2016). MicroRNA-125b-5p mimic inhibits acute liver failure. *Nature Communications*, *7*, 1–11. https://doi.org/10.1038/ncomms11916

Younossi, Z. M., Koenig, A. B., Abdelatif, D., Fazel, Y., Henry, L., & Wymer, M. (2016). Global epidemiology of non-alcoholic fatty liver disease-Meta-analytic assessment of prevalence, incidence and outcomes. *Hepatology*, *64*(1), 73–84. https://doi.org/10.1002/hep.28431

Zhang, J. Y., Kothapalli, K. S. D., & Brenna, J. T. (2016). Desaturase and elongase-limiting endogenous long-chain polyunsaturated fatty acid biosynthesis. *Current Opinion in Clinical Nutrition and Metabolic Care*, *19*(2), 103–110. https://doi.org/10.1097/MCO.0000000000000254

SUPPORTING INFORMATION

Additional supporting information may be found online in the Supporting Information section at the end of the article.